Journal of Physics D: Applied Physics

PAPER

The role of aquaporins in the anti-glioblastoma capacity of the cold plasma-stimulated medium

To cite this article: Dayun Yan *et al* 2017 *J. Phys. D: Appl. Phys.* **50** 055401

The role of aquaporins in the anti-glioblastoma capacity of the cold plasma-stimulated medium

Dayun Yan[1†], Haijie Xiao[2†], Wei Zhu[1], Niki Nourmohammadi[3], Lijie Grace Zhang[1], Ka Bian[2*], and Michael Keidar[1*]

[1]Department of Mechanical and Aerospace Engineering, The George Washington University, Science & Engineering Hall, 800 22nd Street, NW, Room 3550, Washington, DC 20052, USA

[2]Department of Biochemistry and Molecular Medicine, The George Washington University, Ross Hall, 2300 Eye Street, NW, Washington, DC 20037, USA

[3]Department of Biological Sciences, The George Washington University, Lisner Hall, 2023 G Street, NW, Suite 340, Washington, DC 20052, USA

[†]These two authors contribute equally to this research.

*Corresponding authors: Ka Bian bcmkxb@gwu.edu, Michael Keidar keidar@gwu.edu

Abstract. The cold atmospheric plasma (CAP) is a promising novel anti-cancer method. Our previous study showed that the cold plasma-stimulated medium (PSM) exerts remarkable anti-cancer effect as effectively as the direct CAP treatment does. H_2O_2 has been identified as a key anti-cancer substance in PSM. However, the mechanisms underlying intracellular H_2O_2 regulation by cancer cells is largely unknown. Aquaporins (AQPs) are the confirmed membrane channels of H_2O_2. In this study, we first demonstrated that the anti-glioblastoma capacity of PSM could be inhibited by silencing the expression of AQP8 in glioblastoma cells (U87MG) or using the

aquaporins-blocker silver atoms. This discovery illustrates the key intermediate role of AQPs in the toxicity of PSM on cancer cells. Because expression of AQPs varies significantly among different cancer cell lines, this study may facilitate the understanding on the diverse responses of cancer cells to PSM or the direct CAP treatment.

Introduction.

Cancer is one of the largest threats to human health. Developing a novel anti-cancer method with minimal damage to normal cells and tissues is always the goal of scientists. Cold atmospheric plasma (CAP), a near-room temperature ionized gas composed of reactive electrons, ionic, atomic, molecular, and radical species [1], showed a remarkable selective anti-cancer capacity over dozens of cancer cell lines *in vitro* [2-12] and in several animal studies *in vivo* [5, 13-15]. Recently, the direct plasma treatment by the CAP jet or the dielectric barrier discharge (DBD) and the cold plasma-stimulated medium (PSM) has been proved to be a selective anti-cancer method [16-25]. PSM can be stably stored over a wide temperature range, by regulating the component of medium [26] or controlling the storage temperature [27, 28]. PSM can be used as a succedaneum for CAP particularly in the circumstances when some inside tumorous tissues cannot be easily reached by CAP jet.

Understanding the anti-cancer mechanism of CAP is a challenge in plasma medicine. PSM is also named as the indirect CAP treatment. In contrast, the direct CAP treatment denotes the CAP treatment on cells cultured in petri dishes [7, 29, 30] or in multi-wells plates [31-33]. So far, in many cases, the cells were immersed in a layer of cell culture medium during the direct CAP treatment [34-36]. Such layer of medium plays the intermediate role of delivering the plasma-

originated reactive species from gas phase into the aqueous solution and further affecting cells [37]. Thus, understanding anti-cancer mechanism of PSM will also facilitate the understanding on the direct CAP treatment on cancer cells *in vitro*.

So far, among diverse CAP-originated species, H_2O_2, has been proved to be one of main anti-cancer reactive species of PSM [19, 20, 23, 26-28, 38]. Very recently, synergistically using H_2O_2/NO_2^- [22] or $H_2O_2/NO_2^-/NO_3^-$ [25] in medium [22] or phosphate buffered saline (PBS) [25] generated a similar anti-cancer effect as PSM did. Thus, ROS mainly H_2O_2 and RNS mainly NO_2^-/NO_3^- in PSM contribute to the death of cancer cells. RNS in PSM was showed to play a minor anti-cancer role [22, 25]. According to the current conclusions, the anti-cancer mechanism of PSM is largely based on the interaction between ROS mainly H_2O_2 and cancer cells.

Since most of plasma-originated reactive species are either charged or polar molecules, specific channels and transporters on the cytoplasmic membrane are necessary for the transmembrane diffusion of these reactive species. The membrane proteins may be a key to understand the cellular response to the CAP treatment. However, the role of membrane channels of cancer cells in the anti-cancer mechanism of PSM or direct CAP treatment has never been investigated yet. Aquaporins (AQPs) were first discovered as the specific water channel decades ago [39]. Recently, the key role of AQPs in the transmembrane diffusion of several small molecules including H_2O_2, CO_2, NO, NH_3, urea, and glycerol has been unveiled [40]. Among AQPs family, only AQP 1, 3, 8, and 9 have been confirmed as the membrane channels facilitating the H_2O_2 transmembrane diffusion [41-45]. In contrast with AQP1, AQP8 is able to better facilitate the diffusion of H_2O_2 across the cellular membrane of yeast cells [43], which may be partially due to the large average

diameter of the ar/R constriction regions of AQP8 [2, 43]. The yeast cells without AQPs show a strong resistance to high concentration extracellular H_2O_2 [43]. On the contrary, the expression of AQP8 causes a significant yeast cell death upon the treatment of low concentration extracellular H_2O_2 [43]. Thus, AQPs may play a key role in the anti-cancer capacity of PSM particularly in the transmembrane diffusion of plasma-originated H_2O_2.

In this study, we first investigated the expression of AQPs in glioblastoma cells (U87MG). AQP9 show the highest expression among all AQPs. We then inhibited the expression of AQP8 and AQP9 in U87MG cells by siRNA technology and found that the anti-glioblastoma effect of PSM were significantly inhibited by silencing AQP8 but not by silencing AQP9. Corresponding rise of intracellular ROS in U87MG cells were also inhibited by silencing AQP8. We also demonstrated that the anti-glioblastoma capacity of PSM can be significantly inhibited by adding $AgNO_3$ which can block the water channels of AQPs [46, 47]. This study demonstrates that AQPs play a key intermediate role in the anti-cancer capacity of PSM.

Methods.

CAP device. The CAP device was a CAP jet generator using helium as the carrying gas. This CAP jet has been used to study the anti-cancer effect of the direct CAP treatment [30, 48] and PSM [18, 19, 24, 26]. The violet plasma was generated between a ring grounded cathode and a central anode and was ejected out from a quartz tube with a diameter of 4.5 mm. The helium gas flowed at a rate of 4.7 L/min. The input voltage of DC power was 11.5 V. The output voltage was 3.16 kV. The plasma discharge was driven by an alternating current (AC) high voltage with a frequency of 30 kHz. The emission spectrum of CAP has been measured in previous study, demonstrating that

CAP in the gas phase was mainly composed of ROS ($OH^{\cdot}$, O), RNS (NO, N_2^+), and helium (He) [49].

Cell cultures. Standard DMEM was purchased from Life Technologies (11965-118, with L-glutamine). DMEM was mixed with 1% (v/v) antibiotic (penicillin and streptomycin) solution (Life Technologies). Human glioblastoma (U87MG) cells were provided by Dr. Murad's lab at the George Washington University. The media used in the cell seeding process and initial cell culture were composed of DMEM supplemented with 10% (v/v) fetal bovine serum (ThermoFisher Scientific) and 1% (v/v) antibiotic (penicillin and streptomycin) solution (Life Technologies). In each experiment, 6 wells in a single column on 96-well plate were seeded with cancer cells at a concentration of 3 x 10^4 cells/ml in 100 μL and were grown for 8 hours under the standard cell culture conditions (a humidified, 37°C, 5% CO_2 environment). All wells on the margins of 96-well plate have not been used in experiments. When PSM was used to treat glioblastoma cells, the medium which have been used to grow cells for 8 hours were removed first.

cDNA synthesis and quantitative PCR. RNA purification was performed by using TRIzol (ThermoFisher) according to the manufactures' instruction. Briefly, 1 mL of TRIzol was added into U87MG cells of 10^6 grown in culture dish after medium was removed and cells were then scraped from the dish and transferred to eppendorf tube. After 5 min of incubation at room temperature, 200 μL of chloroform was then added into the cell lysate and tube was shook vigorously for about 15 s. After incubation at room temperature for 3 min, the mixture was centrifuged at 12,000 g for 15 min at 40°C. Then 500 μL of isopropanol was added into the aqueous phase and the mixture was incubated at room temperature for 10 min. RNA was

precipitated at 14,000 g for 10 min and then washed with 1 mL 75% ethanol. The precipitated RNA was air dry for 5-10 min and then re-suspended in 50 µL of H_2O.

cDNA was made by using iScript cDNA synthesis kit from Bio-Rad company with 1µg of RNA in 20 µL of reaction under the following condition: incubation at 25ºC for 5 min followed by 42ºC for 30 min and 85ºC for 5 min. Quantitative real time PCR was performed by using SYBR green reagent (Bio-Rad 170-880) with a CFX96 system at the following condition: 95 ºC initial denaturation 3 min followed by 40 cycles of denaturation at 95 ºC for 15 s, annealing and elongation at 60 ºC for 30 s, Primers used in this study are shown in Table 1.

Table 1. Primers of AQPs used in this study. F: forward; R: Reverse.

Genes	Sequence (5'-3')	Expected PCR product size (bp)
AQP1	**F:** CCTGGCTATTGACTACAC; **R:** GAAGTCGTAGATGAGTACA.	147
AQP2	**F:** CCACCTCCTTGGGATCCATTA; **R:** AGGGGTCCGATCCAGAAGAC.	114
AQP3	**F:** ACCAGCTTTTTGTTTCGGGC; **R:** GGCTGTGCCTATGAACTGGT.	110
AQP4	**F:** ACTGGTGCCAGCATGAATCC; **R:** GGGCCCAACCCAATATATCCAA.	90
AQP5	**F:** GCTCACTGGGTTTTCTGGGTA; **R:** CCTCGTCAGGCTCATACGTG.	139
AQP6	**F:** TCGTAGGCTCCCACATCTCT; **R:** CTGTTCCGGACCACGTTGAT.	145
AQP7	**F:** GGACAGTCACGGAGGAACAA; **R:** TCAGATTTGTAGATGTCTGCTGAA.	102
AQP8	**F:** GTGCCTGTCGGTCATTGAGA; **R:** CAGGGTTGAAGTGTCCACCA.	125
AQP9	**F:** TCCTCAGAGAAGCCCCAAGA; **R:** AGCCACATCCAAGGACAATCA.	146
AQP10	**F:** TGTTTGTACTCATGCAGCTCCT; **R:** GGCTATCGTAACGGCCAGAG.	119
AQP11	**F:** CCAGGAAGTCCGAACCAAGC; **R:** CCTGTTAGACTTCCTCCTGCATA.	84
AQP12	**F:** TGGCAGGTCTTAACGTGTCC; **R:** CAGCGTCCTCATCGCCTC.	13

AQP8 and AQP9 knockdown. The on-target plus smartpool siAQP8 and siAQP9 were purchased from Dharmacon and siRNA transfection was performed by using Lipofectamine RNAiMAX

(Invitorgen 13778) according to the manufactures' instruction. Basically, U87MG cells grown to 50% confluence in 6-well culture dish were washed with OPTI low serum medium (Invitrogen, 31985) and then transfected with 4 μL of siAQP8 or siAQP9 (10 μM) together with 4 μL of Lipofectamine RNAiMAX in OPTI medium for each well. Universal negative control siRNA (Sigma, sic001) was used as a negative control. After 6 hr of transfection, cells were changed back to DMEM medium which was supplemented with 10% FBS. Quantitative real time PCR was then performed to confirm the AQP8 and AQP9 genes expression.

Making PSM and affecting the growth of glioblastoma cells. The DMEM used in this study was made by mixing 1% (v/v) penicillin-streptomycin (Life Technologies) with standard DMEM (11965-118, Life Technologies). During the CAP treatment, 1 mL of DMEM in a well of 12-well plate was treated by CAP for a specific time length. The gap between the bottom of 12-well plate and the source of CAP was 3 cm. After that, 100 μL of plasma-stimulated DMEM was used to affect the growth of U87MG cells in each well immediately. The control group was the case that U87MG cells cultured in DMEM without the CAP treatment. The sample number in each case was 6. Thus, only 600 μL in each 1 mL of plasma-stimulated DMEM were transferred to affect U87MG cells. Glioblastoma cells were cultured for 2 days before the cell viability was measured by MTT assay. The sextuplicate experiments were independently repeated for twice.

Measuring H_2O_2 concentration in DMEM. The H_2O_2 concentration in PSM was measured by using Fluorimetric Hydrogen Peroxide Assay Kit (Sigma-Aldrich) according to the protocols provided by manufacturer. A H1 microplate reader (Hybrid Technology) was used to measure the fluorescence with an excitation wavelength at 540 nm and an emission wavelength at 590 nm. The

final fluorescent strength of the experimental group was obtained by deducting the measured fluorescent strength of the control group from the measured fluorescent strength of the experimental group. The standard H_2O_2 solution (Sigma-Aldrich) was used to prepare the standard H_2O_2 concentration-fluorescence curve. Based on this standard concentration-fluorescence curve, the H_2O_2 concentration in the plasma-treated DMEM was obtained.

Making the H_2O_2-rich DMEM and affecting the growth of glioblastoma cells. The H_2O_2-rich DMEM was prepared by mixing 30 wt % (9.8 M) H_2O_2 solution (Sigma-Aldrich) with DMEM (11965-118, Life Technologies). 18.13 μM, 36.26 μM, 54.39 μM, and 72.52 μM H_2O_2-rich DMEM were prepared according to the H_2O_2 concentration in the 0.5 min, 1 min, 1.5 min, and 2 min of CAP-stimulated DMEM. 100 μL of H_2O_2-rich DMEM was transferred to affect the growth of U87MG cells in each well immediately. The control group was the case that U87MG cells cultured in DMEM without the CAP treatment. The sample number in each case was 6. Thus, only 600 μL in 1 mL of plasma-stimulated DMEM were transferred to affect U87MG cells. U87MG cells were cultured for 2 days before the measurement of cell viability using MTT assay. The sextuplicate experiments were independently repeated for twice.

Making the CAP-stimulated $AgNO_3$-rich DMEM and affecting the growth of glioblastoma cells. The $AgNO_3$-rich DMEM was prepared by mixing 0.01 M silver nitrate solution (Sigma-Aldrich) with DMEM. During the CAP treatment, 1 mL of medium (DMEM or $AgNO_3$-rich DMEM) in a well of 12-well plate was treated by CAP for 1 min. The gap between the bottom of 12-well plate and the bottom edge of quartz tube was 3 cm. After that, 100 μL of plasma-stimulated medium (DMEM or $AgNO_3$-rich DMEM) was transferred to affect the growth of U87MG cells in

each well immediately. The control group was the case that U87MG cells cultured in the medium (DMEM or $AgNO_3$-rich DMEM) without the CAP treatment. The sample number of each case was 6. U87MG cells were cultured for 3 days before the cell viability was measured. The sextuplicate experiments were independently repeated for three times.

Cell viability measurement, data and statistics processing. According to the protocols provided by manufacturer, the MTT (3-(4,5-Dimethylthiazol-2-yl)-2,5-Diphenyltetrazolium Bromide) assay was performed. The original experimental data about the cell viability was the absorbance at 570 nm measured by a H1 microplate reader (Hybrid Technology). To facilitate analyzing data, the original measured cell viability was processed to be the relative cell viability through the division between the measured cell viability (absorbance) of U87MG cells cultured in plasma-stimulated DMEM or H_2O_2-rich DMEM to the measured cell viability of U87MG cells cultured in the untreated DMEM. The measured cell viability of each experiment was equal to the mean value of 6 samples from 6 wells. The final data shown in this manuscript were the mean ± s.d. of two independently repeated experiments.

Intracellular ROS measurement. The intracellular ROS in the U87MG cells were measured by using DCFDA-Cellular Reactive Oxygen Species Detection Assay Kit (113851, Abcam). U87MG cells were seeded in 35 mm easy grip culture dish with a confluence of 4 x 10^4 cells/mL. In each dish, 2 mL of medium (90% v/v DMEM and 10% v/v FBS) were used to culture U87MG cells for 5 hours in the incubator under the standard culture conditions. 12 mL of 25 μM DCFDA solution was prepared by mixing 18 μL of 20 mM DCFDA solution with 12 mL of 1X buffer. After 4 hours of incubation, the medium in 35 mm dish were removed. 1 mL of 1X buffer was used to wash the

cells in dish. 2 mL of 25 μM DCFDA solution were used to culture U87MG cells for 40 min in the incubator under the standard culture conditions. 1 mL of 1X buffer was used to wash the cells in dish. The cells from control group and experiments groups were finally cultured for 2 hours in the DMEM without CAP treatment and the CAP-stimulated DMEM, respectively. The CAP-stimulated DMEM was made by treating 1 mL of DMEM in a well of 12-well plate for 4 min. Finally, the fluorescent signal of cells in 35 mm dish was detected by a laser scanning confocal microscope with an excitation wavelength at 488 nm (Zeiss, LSM 710).

Results and discussion.

The expression of AQPs in tumor tissues has been widely investigated in past decades [50, 51]. The expression of AQP1 [52-54], AQP8 [55], and AQP9 [56-58] in glioblastoma tissues have been confirmed. However, the expression of AQPs in glioblastoma cell lines (U87MG) have not been investigated yet. We first investigated the expression style of AQPs family in U87MG cells. Our PCR analysis of AQPs family (AQP1-AQP12) showed that only AQP1, AQP3, AQP5, AQP7, AQP8, AQP9, and AQP11 are expressed in U87MG cells (Fig. 1a). Among these AQPs, the expression of AQP9 is the most abundant. AQP9 is reported to play important roles in the malignant progression of brain astrocytic tumors [56], such as counteracting the glioma-associated lactic acidosis by clearance of glycerol and lactate from the extracellular space [57]. AQP9 has been proposed to be a new biomarker in glioblastoma diagnosis and a new target for glioblastoma therapy [56]. So far, only AQP1, AQP3, AQP8, and AQP9 have been reported as the H_2O_2 transmembrane channels [41-45]. In addition, AQP8 has been regarded as the most efficient H_2O_2 channels among these four AQPs [2, 43]. Thus, AQP8 and AQP9 were chosen to study AQPs' role in anti-glioblastoma effect of PSM by using siRNA technology. Compared with the control

group (sicontrol), the expression of AQP8 (Fig. 1b) and AQP9 (Fig. 1c) in U87MG cells decreased about 80% and 90% 48 hours after the transfection, respectively. The silencing of AQP8 and AQP9 by siRNA is highly time-sensitive. The expression of AQP8 and AQP9 were lowest 48 hours after the transfection. Their expression began to recover 72 hours after the transfection.

To investigate the role of AQP8 and AQP9 in the anti-glioblastoma capacity of PSM, U87MG cells with a repressed expression of AQP8 and AQP9 were cultured in the CAP-stimulated DMEM or H_2O_2-rich DMEM without the CAP treatment. The detailed description for the protocols is illustrated in Methods. For both two treatments, the anti-glioblastoma capacity of PSM increases when the treatment time in PSM increases (Fig. 2a) or the concentration of H_2O_2 in H_2O_2-rich DMEM increase (Fig. 2b). This trend is consistent with our previous reports about the application of PSM on glioblastoma cells treatment [18, 19, 24]. The anti-glioblastoma effect of PSM will not be obvious until the treatment time of CAP is adequately long (Fig. 2a) or the concentration of H_2O_2 is adequately high (Fig. 2b). Knockdown of AQP8 but not AQP9 in U87MG cells can significantly reduce the anti-glioblastoma capacity of PSM (Fig. 2a) and the toxicity of H_2O_2-rich DMEM (Fig. 2b). This trend is consistent with the previous conclusion that AQP8 is an efficient H_2O_2 transmembrane channel [2, 43]. The comparative study about the H_2O_2 transmembrane diffusion efficiency of AQP8 and AQP9 is still lacking in biology. Despite AQP9 is most expressed in U87MG cells, its transmembrane diffusion efficiency for H_2O_2 may be much less than AQP8. The estimated diameter of the ar/R constriction region of AQP8 is much larger than AQP0, 1, 2, 4, and 5 [2]. AQP8 may be the most efficient H_2O_2 channels among AQP1, 3, and 9. In addition, so far, dozens of references about the roles of AQP1, 3, and 8 as the H_2O_2 channels have been reported [59]. However, only one report has demonstrated that AQP9 is a H_2O_2 channels

recently. In biology, it may be still disputable to conclude that AQP9 is a H_2O_2 channel. Probably, due to above reasons, just inhibiting AQP9 but not AQP8 does not result in a noticeable change on the anti-glioblastoma effect of PSM on U87MG cells. AQP8 still worked when we just silenced AQP9. Clearly, a more comprehensive study on the role of each member of AQP in the anti-cancer capacity of PSM should be performed in the further investigation. Nonetheless, silencing specific AQP in U87MG cells indeed weakens the anti-cancer effect of PSM.

The weakened anti-glioblastoma capacity of PSM by inhibiting the expression of AQP8 can be due to the weakened transmembrane diffusion of H_2O_2 in U87MG cells. Then, the rise of intracellular ROS in U87MG cells should also be decreased when the expression of AQP8 is inhibited. To confirm this, intracellular ROS fluorescent detection measurement was performed. We observed that the noticeable rise of intracellular ROS in the PSM-treated U87MG cells disappeared when the expression of AQP8 was inhibited in U87MG cells (Fig. 2c). Thus, AQP8 plays a key intermediate role in the transmembrane diffusion of plasma-originated H_2O_2 in U87MG cells. The expression level of specific AQPs in cancer cells may be an important factor in determining the anti-cancer capacity of PSM.

To inhibit the function of AQPs, pharmacological agents such as bumetanide and furosemide [60], as well as metal atoms such as gold (Au), mercury (Hg), and silver (Ag) [61] have been widely used as the AQPs-blockers. The blocking mechanism of mercury atom in the channel of AQPs have been investigated through analyzing the crystal structure of AQPs tetramers with a mercury atom in each monomer [62]. Silver and other atoms such as gold may block the channel of AQPs using similar mechanism, though the corresponding structural biology data are still lacking. We

have used silver rather than mercury was based on two reasons. First, mercury and corresponding chemicals with mercury such as mercury chloride evaporate during the standard cell culture conditions, which rises a potential safety risk to researchers. Second, silver atoms show a better AQPs-blocking property than mercury atoms [61]. For the erythrocytes, 10 μM Ag^+ already causes about 80% inhibition on water transportation capacity [61]. Inhibiting the transmembrane diffusion of H_2O_2 in leukemia (B1647) cells by 5 μM $AgNO_3$ have been demonstrated recently [63].

In this study, the anti-glioblastoma capacity of the CAP-stimulated $AgNO_3$-rich DMEM and DMEM was compared. As shown in Fig. 3a, the noticeable anti-glioblastoma effect of the PSM gradually decreases as the concentration of $AgNO_3$ in DMEM increases from 2 μM to 10 μM. Compared with the effect of silencing AQP8 on the anti-glioblastoma capacity of PSM, $AgNO_3$ shows a stronger interference on the anti-glioblastoma capacity of PSM. This phenomenon may be due to two main faults of $AgNO_3$ compared with siRNA technology. First, silver does not target a specific AQPs but may block different AQPs. It is possible that both AQP1, 3, 8, or 9 have been blocked by silver atoms. On the contrary, we have not inhibited the expression of AQP1 or AQP3 in this study. It is possible that AQP1 and AQP3 also partially contribute to the transmembrane diffusion of H_2O_2. Second, $AgNO_3$ may affect other cellular pathways to U87MG cells other than just blocking AQPs. For example, silver may react with H_2O_2 and form hydroxyl radical, which is highly reactive with many key molecules including proteins and DNA [64].

Obviously, $AgNO_3$-rich DMEM with a high concentration (>10 μM) was very toxic to U87MG cells (Fig. 3a). Because NO_3^- with such a low concentration is not toxic to cancer cells [25], the toxicity of $AgNO_3$-rich DMEM should be mainly due to silver. Silver may react with chloride in

DMEM to form silver chloride sediment. However, the noticeable toxicity of $AgNO_3$ on U87MG cells demonstrate that significant silver still dissolves in DMEM. The concentration of H_2O_2 in the CAP-stimulated AgNO3-rich DMEM has also been measured by using Fluorimetric Hydrogen Peroxide Assay Kit. The increased $AgNO_3$ concentration in DMEM does not decrease the generation of H_2O_2 in the CAP-stimulated DMEM (Fig. 3b). Because H_2O_2 is the main anti-cancer reactive species in PSM, the weakened anti-cancer effect of PSM is not due to the consumptive reaction between H_2O_2 and silver.

Different tumor tissues express AQPs with quite different levels [50, 51]. Thus, this study provides a clue to understand the different response of cancer cells to the CAP treatment *in vitro*. For example, it is found that cancer cells with higher proliferation rate are more sensitive to the CAP treatment than the cancer cells with lower proliferation rate [65]. Actually, it is also found that the cancer cells from the high tumorigenic stage tend to express more AQPs than cancer cells from the low tumorigenic stage [55]. The high AQPs expression in cancer cells from the high tumorigenic stage may explain the strong sensitivity of these cancer cells to the CAP treatment.

Conclusions.

Aquaporins, the only confirmed transmembrane channels of H_2O_2, play a key intermediate role in the anti-glioblastoma effect of PSM. Inhibiting the expression of AQP8 in U87MG cells or using aquaporins-blocker silver atoms significantly weaken the anti-glioblastoma capacity of PSM. Expression level of aquaporins family in cancer cells significantly affect the anti-cancer effect of PSM. Because aquaporins are widely but diversely expressed in cancer cells, this study provides a novel framework to understand the different responses of cancer cells to the CAP treatment.

Acknowledgements. This work was supported in part by GW Institute of Nanotechnology and National Science Foundation, grant 1465061.

References.

[1] Lu X, Naidis GV, Laroussi M, Reuter S, Graves DB, Ostrikov K. Reactive species in non-equilibrium atmospheric-pressure plasmas: Generation, transport, and biological effects. Physics Reports. 2016;630:1-84.

[2] Yan D, Talbot A, Nourmohammadi N, Sherman JH, Cheng X, Keidar M. Toward understanding the selective anticancer capacity of cold atmospheric plasma—A model based on aquaporins (Review). Biointerphases. 2015;10:040801.

[3] Georgescu N, Lupu AR. Tumoral and normal cells treatment with high-voltage pulsed cold atmospheric plasma jets. Plasma Science, IEEE Transactions on. 2010;38:1949-55.

[4] Kim GJ, Kim W, Kim KT, Lee JK. DNA damage and mitochondria dysfunction in cell apoptosis induced by nonthermal air plasma. Applied Physics Letters. 2010;96:021502.

[5] Keidar M, Walk R, Shashurin A, Srinivasan P, Sandler A, Dasgupta S, et al. Cold plasma selectivity and the possibility of a paradigm shift in cancer therapy. British journal of cancer. 2011;105:1295-301.

[6] Keidar M. Plasma for cancer treatment. Plasma Sources Science and Technology. 2015;24:033001.

[7] Fridman G, Shereshevsky A, Jost MM, Brooks AD, Fridman A, Gutsol A, et al. Floating Electrode Dielectric Barrier Discharge Plasma in Air Promoting Apoptotic Behavior in Melanoma Skin Cancer Cell Lines. Plasma Chemistry and Plasma Processing. 2007;27:163-76.

[8] Yan X, Xiong Z, Zou F, Zhao S, Lu X, Yang G, et al. Plasma-Induced Death of HepG2 Cancer Cells: Intracellular Effects of Reactive Species. Plasma Processes and Polymers. 2012;9:59-66.

[9] Zhao S, Xiong Z, Mao X, Meng D, Lei Q, Li Y, et al. Atmospheric pressure room temperature plasma jets facilitate oxidative and nitrative stress and lead to endoplasmic reticulum stress dependent apoptosis in HepG2 cells. PloS one. 2013;8:e73665.

[10] Keidar M, Shashurin A, Volotskova O, Ann Stepp M, Srinivasan P, Sandler A, et al. Cold atmospheric plasma in cancer therapy. Physics of Plasmas. 2013;20:057101.

[11] Zhu W, Lee SJ, Castro NJ, Yan D, Keidar M, Zhang LG. Synergistic Effect of Cold Atmospheric Plasma and Drug Loaded Core-shell Nanoparticles on Inhibiting Breast Cancer Cell Growth. Scientific reports. 2016;6:21974.

[12] Yan D, Sherman JH, Keidar M. Cold atmospheric plasma, a novel promising anti-cancer treatment modality. Oncotarget. 2016; Epub ahead of print.

[13] Vandamme M, Robert E, Dozias S, Sobilo J, Lerondel S, Le Pape A, et al. Response of human glioma U87 xenografted on mice to non thermal plasma treatment. Plasma medicine. 2011;1:27-43.

[14] Brulle L, Vandamme M, Ries D, Martel E, Robert E, Lerondel S, et al. Effects of a non thermal plasma treatment alone or in combination with gemcitabine in a MIA PaCa2-luc orthotopic pancreatic carcinoma model. PloS one. 2012;7:e52653.
[15] Walk RM, Snyder JA, Srinivasan P, Kirsch J, Diaz SO, Blanco FC, et al. Cold atmospheric plasma for the ablative treatment of neuroblastoma. Journal of pediatric surgery. 2013;48:67-73.
[16] Tanaka H, Mizuno M, Ishikawa K, Nakamura K, Kajiyama H, Kano H, et al. Plasma-Activated Medium Selectively Kills Glioblastoma Brain Tumor Cells by Down-Regulating a Survival Signaling Molecule, AKT Kinase. Plasma Medicine. 2011;1:265-277.
[17] Utsumi F, Kajiyama H, Nakamura K, Tanaka H, Mizuno M, Ishikawa K, et al. Effect of indirect nonequilibrium atmospheric pressure plasma on anti-proliferative activity against chronic chemo-resistant ovarian cancer cells in vitro and in vivo. PloS one. 2013;8:e81576.
[18] Yan D, Sherman JH, Cheng X, Ratovitski E, Canady J, Keidar M. Controlling plasma stimulated media in cancer treatment application. Applied Physics Letters. 2014;105:224101.
[19] Yan D, Talbot A, Nourmohammadi N, Cheng X, Canady J, Sherman J, et al. Principles of using Cold Atmospheric Plasma Stimulated Media for Cancer Treatment. Scientific reports. 2015;5:18339.
[20] Mohades S, Laroussi M, Sears J, Barekzi N, Razavi H. Evaluation of the effects of a plasma activated medium on cancer cells. Physics of Plasmas. 2015;22:122001.
[21] Kumar N, Park JH, Jeon SN, Park BS, Choi EH, Attri P. The action of microsecond-pulsed plasma-activated media on the inactivation of human lung cancer cells. Journal of Physics D: Applied Physics. 2016;49:115401.
[22] Kurake N, Tanaka H, Ishikawa K, Kondo T, Sekine M, Nakamura K, et al. Cell survival of glioblastoma grown in medium containing hydrogen peroxide and/or nitrite, or in plasma-activated medium. Arch Biochem Biophys. 2016;605:102-108.
[23] Adachi T, Nonomura S, Horiba M, Hirayama T, Kamiya T, Nagasawa H, et al. Iron stimulates plasma-activated medium-induced A549 cell injury. Scientific reports. 2016;6:20928.
[24] Yan D, Nourmohammadi N, Talbot A, Sherman JH, Keidar M. The strong anti-glioblastoma capacity of the plasma-stimulated lysine-rich medium. Journal of Physics D: Applied Physics. 2016;49:274001.
[25] Girard PM, Arbabian A, Fleury M, Bauville G, Puech V, Dutreix M, et al. Synergistic Effect of H2O2 and NO2 in Cell Death Induced by Cold Atmospheric He Plasma. Scientific reports. 2016;6:29098.
[26] Yan D, Nourmohammadi N, Bian K, Murad F, Sherman JH, Keidar M. Stabilizing the cold plasma-stimulated medium by regulating medium's composition. Scientific reports. 2016;6:26016.
[27] Adachi T, Tanaka H, Nonomura S, Hara H, Kondo S, Hori M. Plasma-activated medium induces A549 cell injury via a spiral apoptotic cascade involving the mitochondrial-nuclear network. Free radical biology & medicine. 2014;79C:28-44.
[28] Judee F, Fongia C, Ducommun B, Yousfi M, Lobjois V, Merbahi N. Short and long time effects of low temperature Plasma Activated Media on 3D multicellular tumor spheroids. Scientific reports. 2016;6:21421.
[29] Kim SJ, Chung TH, Bae SH, Leem SH. Induction of apoptosis in human breast cancer cells by a pulsed atmospheric pressure plasma jet. Applied Physics Letters. 2010;97:023702.

[30] Shashurin A, Stepp MA, Hawley TS, Pal-Ghosh S, Brieda L, Bronnikov S, et al. Influence of Cold Plasma Atmospheric Jet on Surface Integrin Expression of Living Cells. Plasma Processes and Polymers. 2010;7:294-300.
[31] Kim JY, Ballato J, Foy P, Hawkins T, Wei Y, Li J, et al. Apoptosis of lung carcinoma cells induced by a flexible optical fiber-based cold microplasma. Biosensors & bioelectronics. 2011;28:333-8.
[32] Barekzi N, Laroussi M. Dose-dependent killing of leukemia cells by low-temperature plasma. Journal of Physics D: Applied Physics. 2012;45:422002.
[33] Kaushik N, Kaushik NK, Kim CH, Choi EH. Oxidative Stress and Cell Death Induced in U-937 Human Monocytic Cancer Cell Line by Non-Thermal Atmospheric Air Plasma Soft Jet. Science of Advanced Materials. 2014;6:1740-51.
[34] Kaushik NK, Kaushik N, Park D, Choi EH. Altered Antioxidant System Stimulates Dielectric Barrier Discharge Plasma-Induced Cell Death for Solid Tumor Cell Treatment. PloS one. 2014;9:e103349.
[35] Gibson AR, McCarthy HO, Ali AA, O'Connell D, Graham WG. Interactions of a Non-Thermal Atmospheric Pressure Plasma Effluent with PC-3 Prostate Cancer Cells. Plasma Processes and Polymers. 2014;11:1142-1149.
[36] Kang SU, Cho JH, Chang JW, Shin YS, Kim KI, Park JK, et al. Nonthermal plasma induces head and neck cancer cell death: the potential involvement of mitogen-activated protein kinase-dependent mitochondrial reactive oxygen species. Cell death & disease. 2014;5:e1056.
[37] Tanaka H, Mizuno M, Toyokuni S, Maruyama S, Kodera Y, Terasaki H, et al. Cancer therapy using non-thermal atmospheric pressure plasma with ultra-high electron density. Physics of Plasmas. 2015;22:122004.
[38] Yokoyama M, Johkura K, Sato T. Gene expression responses of HeLa cells to chemical species generated by an atmospheric plasma flow. Biochem Biophys Res Commun. 2014;450:1266-71.
[39] Borgnia M, Nielsen S, Engel A, Agre P. Cellular and molecular biology of the aquaporin water channels. Annual review of biochemistry. 1999;68:425-58.
[40] Wu B, Beitz E. Aquaporins with selectivity for unconventional permeants. Cellular and molecular life sciences. 2007;64:2413-21.
[41] Bienert GP, Chaumont F. Aquaporin-facilitated transmembrane diffusion of hydrogen peroxide. Biochimica et Biophysica Acta (BBA)-General Subjects. 2014;1840:1596-604.
[42] Miller EW, Dickinson BC, Chang CJ. Aquaporin-3 mediates hydrogen peroxide uptake to regulate downstream intracellular signaling. Proceedings of the National Academy of Sciences. 2010;107:15681-6.
[43] Almasalmeh A, Krenc D, Wu B, Beitz E. Structural determinants of the hydrogen peroxide permeability of aquaporins. The FEBS journal. 2014;281:647-56.
[44] Watanabe S, Moniaga CS, Nielsen S, Hara-Chikuma M. Aquaporin-9 facilitates membrane transport of hydrogen peroxide in mammalian cells. Biochemical and biophysical research communications. 2016;471:191-7.
[45] Herrera M, Hong NJ, Garvin JL. Aquaporin-1 transports NO across cell membranes. Hypertension. 2006;48:157-64.
[46] Yang B, Kim JK, Verkman A. Comparative efficacy of HgCl2 with candidate aquaporin‐1 inhibitors DMSO, gold, TEA+ and acetazolamide. FEBS letters. 2006;580:6679-84.
[47] Niemietz CM, Tyerman SD. New potent inhibitors of aquaporins: silver and gold compounds inhibit aquaporins of plant and human origin. FEBS letters. 2002;531:443-7.

[48] Volotskova O, Hawley TS, Stepp MA, Keidar M. Targeting the cancer cell cycle by cold atmospheric plasma. Scientific reports. 2012;2:636.
[49] Cheng X, Sherman J, Murphy W, Ratovitski E, Canady J, Keidar M. The Effect of Tuning Cold Plasma Composition on Glioblastoma Cell Viability. PloS one. 2014;9:e98652.
[50] Verkman A, Hara-Chikuma M, Papadopoulos MC. Aquaporins—new players in cancer biology. Journal of molecular medicine. 2008;86:523-9.
[51] Papadopoulos MC, Saadoun S. Key roles of aquaporins in tumor biology. Biochimica et Biophysica Acta (BBA)-Biomembranes. 2015;1848:2576-83.
[52] El Hindy N, Bankfalvi A, Herring A, Adamzik M, Lambertz N, Zhu Y, et al. Correlation of aquaporin-1 water channel protein expression with tumor angiogenesis in human astrocytoma. Anticancer research. 2013;33:609-13.
[53] Oshio K, Binder DK, Liang Y, Bollen A, Feuerstein B, Berger MS, et al. Expression of the Aquaporin-1 Water Channel in Human Glial Tumors. Neurosurgery. 2005;56:375-81.
[54] Deb P, Pal S, Dutta V, Boruah D, Chandran VM, Bhatoe HS. Correlation of expression pattern of aquaporin-1 in primary central nervous system tumors with tumor type, grade, proliferation, microvessel density, contrast-enhancement and perilesional edema. Journal of cancer research and therapeutics. 2012;8:571.
[55] Zhu SJ, Wang KJ, Gan SW, Xu J, Xu SY, Sun SQ. Expression of aquaporin8 in human astrocytomas: correlation with pathologic grade. Biochem Biophys Res Commun. 2013;440:168-72.
[56] Tan G, Sun S, Yuan D. Expression of the water channel protein aquaporin-9 in human astrocytic tumours: correlation with pathological grade. Journal of International Medical Research. 2008;36:777-82.
[57] Warth A, Mittelbronn M, Hülper P, Erdlenbruch B, Wolburg H. Expression of the water channel protein aquaporin-9 in malignant brain tumors. Applied Immunohistochemistry & Molecular Morphology. 2007;15:193-8.
[58] Jelen S, Parm Ulhøi B, Larsen A, Frøkiær J, Nielsen S, Rützler M. AQP9 expression in glioblastoma multiforme tumors is limited to a small population of astrocytic cells and CD15 (+)/CalB (+) leukocytes. PloS one. 2013;8:e75764.
[59] Bienert GP, Chaumont F. Aquaporin-facilitated transmembrane diffusion of hydrogen peroxide. Biochimica et biophysica acta. 2014;1840:1596-604.
[60] Devuyst O, Yool AJ. Aquaporin-1: new developments and perspectives for peritoneal dialysis. Peritoneal dialysis international : journal of the International Society for Peritoneal Dialysis. 2010;30:135-41.
[61] Yang B, Kim JK, Verkman AS. Comparative efficacy of HgCl2 with candidate aquaporin-1 inhibitors DMSO, gold, TEA+ and acetazolamide. FEBS Lett. 2006;580:6679-84.
[62] Savage DF, Stroud RM. Structural basis of aquaporin inhibition by mercury. Journal of molecular biology. 2007;368:607-17.
[63] Vieceli Dalla Sega F, Zambonin L, Fiorentini D, Rizzo B, Caliceti C, Landi L, et al. Specific aquaporins facilitate Nox-produced hydrogen peroxide transport through plasma membrane in leukaemia cells. Biochimica et biophysica acta. 2014;1843:806-14.
[64] He D, Miller CJ, Waite TD. Fenton-like zero-valent silver nanoparticle-mediated hydroxyl radical production. Journal of Catalysis. 2014;317:198-205.

[65] Naciri M, Dowling D, Al-Rubeai M. Differential Sensitivity of Mammalian Cell Lines to Non-Thermal Atmospheric Plasma. Plasma Processes and Polymers. 2014;11:391-400.

Figures

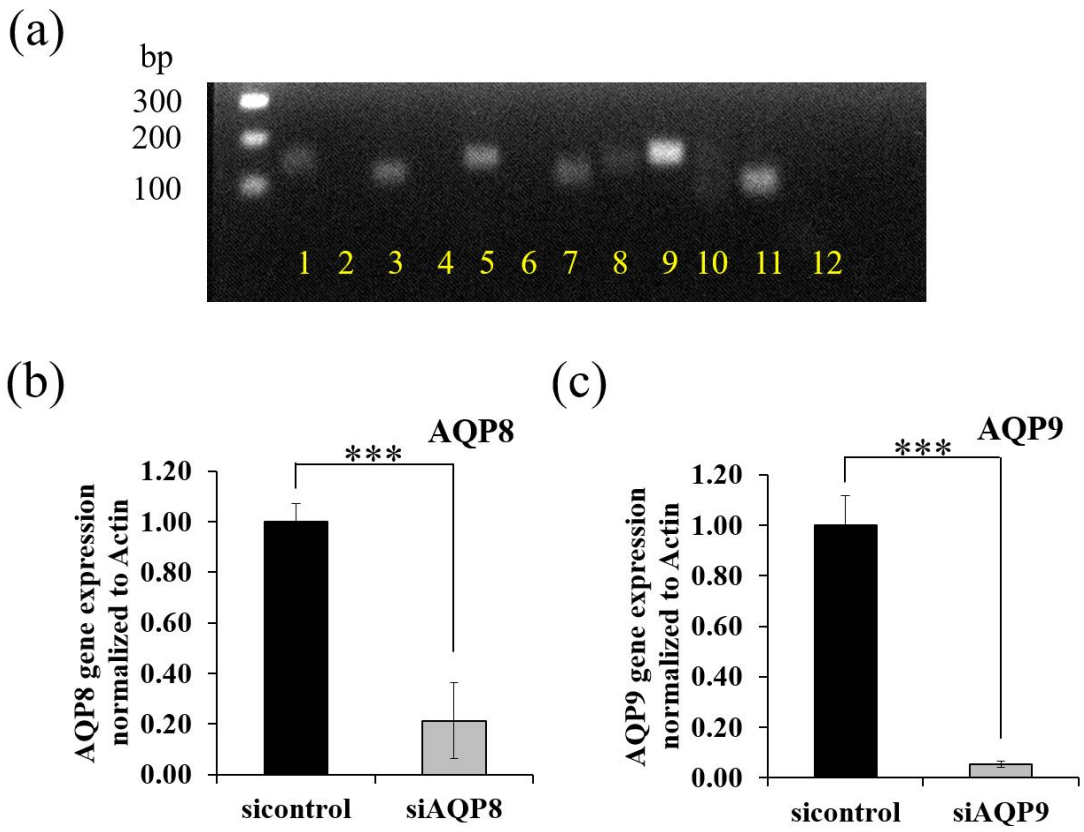

Figure 1. The expression of AQPs in U87MG cells and the inhibited expression of AQP8 and AQP9 by siRNA. (a) RT-PCR analysis of AQP1-AQP12 expression in U87MG cells. cDNA of U87MG cells was used as PCR template and the PCR products were resolved in agarose gel (see Table 1 for predicted PCR products size). (b) Quantitative RT-PCR analysis of expression of AQP8 and AQP9 after siRNA knockdown. RNA was prepared from U87MG cells after knockdown of AQP8 or AQP9 for 48 hr. A universal negative siRNA was used as a control (sicontrol). And then cDNA was synthesized and used as template for PCR. The expression of AQP8 and AQP9 was normalized to the expression of Actin. The results were an average of three different repeats. Student's t-test was performed and the significance is indicated as *** $p < 0.005$, ** $p < 0.01$, and * $p < 0.05$.

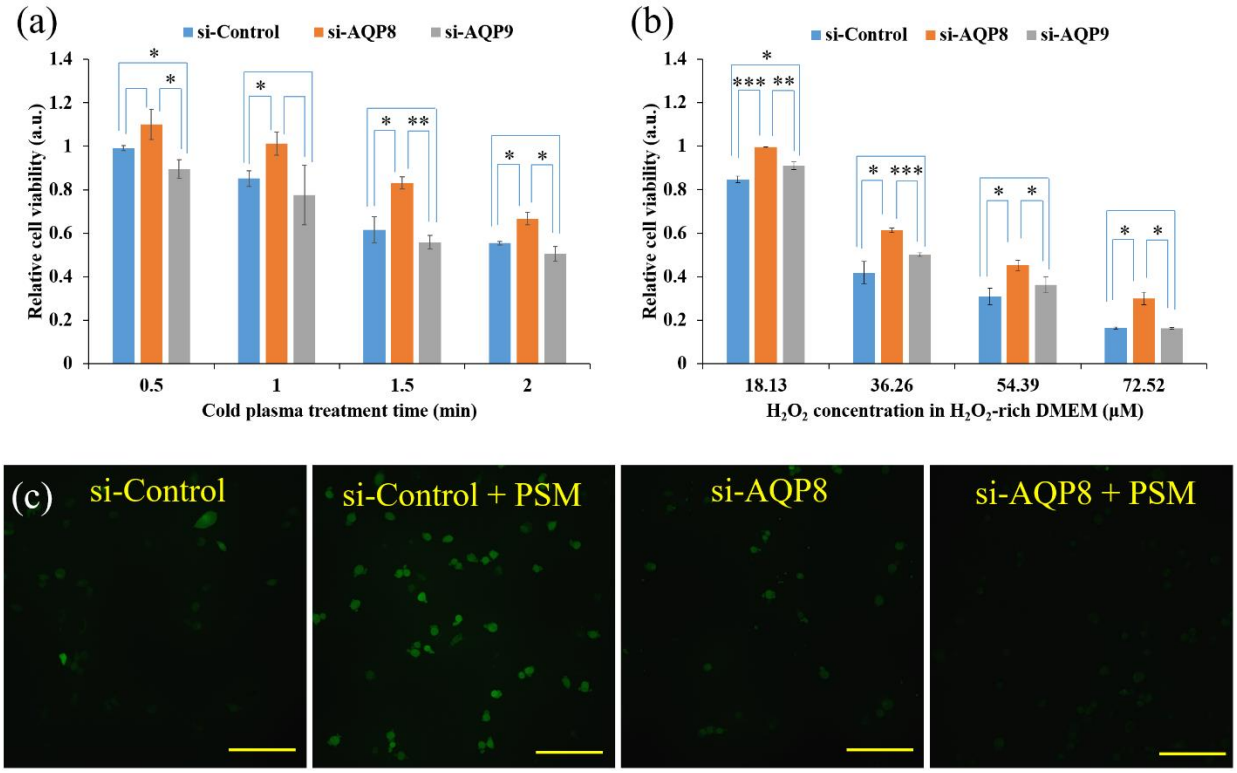

Figure 2. Silencing the expression of AQP8 significantly weakens the anti-glioblastoma capacity of PSM. The anti-glioblastoma capacity of PSM (a) and H_2O_2-rich DMEM (b) on U87MG cells (sicontrol, siAQP8, and siAQP9). Results are presented as the mean ± s.d. of two independently repeated experiments performed in sextuplicate. Student's t-test was performed and the significance is indicated as *** $p < 0.005$, ** $p < 0.01$, and * $p < 0.05$. (c) The rise of intracellular reactive oxygen species (ROS) in U87MG cells (si-control and si-AQP8) was measured by DCFDA-Cellular Reactive Oxygen Species Detection Assay Kit using laser scanning confocal microscope. Scale bar = 100 μm.

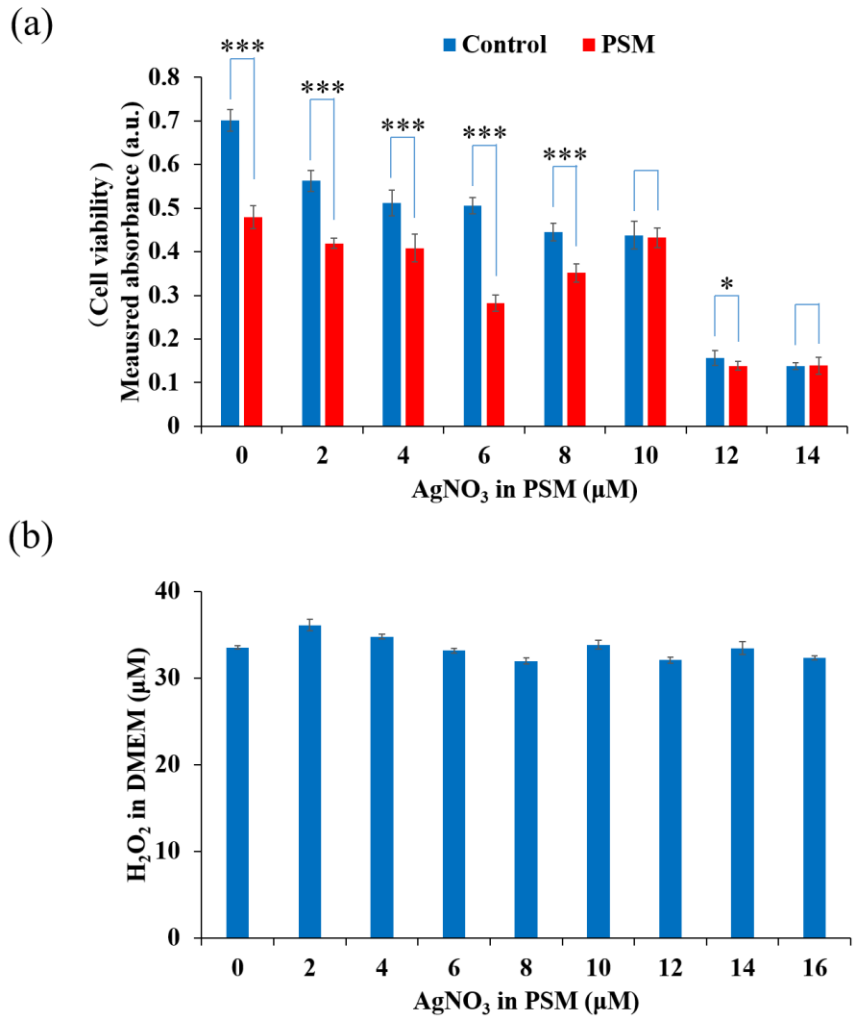

Figure 3. $AgNO_3$ weakens the anti-glioblastoma capacity of PSM. (a) The anti-glioblastoma capacity of the CAP-stimulated $AgNO_3$-rich DMEM (2 - 14 μM) and DMEM (0 μM). The control group represents the case that U87MG cells cultured in the untreated DMEM or in the untreated $AgNO_3$-rich DMEM. Results are presented as the mean ± s.d. of experiments performed in sextuplicate. Student's t-test was performed and the significance is indicated as *** $p < 0.005$, ** $p < 0.01$, and * $p < 0.05$. (b) The generation of H_2O_2 in the CAP-stimulated $AgNO_3$-rich DMEM (2 – 16 μM) and DMEM (0 μM). Results are presented as the mean ± s.d. of three repeated experiments.